BEAM DIAGNOSTICS FOR COMMISSIONING AND OPERATION OF THE FAIR PROTON LINAC

T. Sieber[†], P. Forck, S. Udrea, GSI, Darmstadt, Germany
J. Herranz, A. Vizcaino-de-Julian, PROACTIVE, Barcelona, Spain

Abstract

For the planned antiproton experiments at FAIR a dedicated proton injector Linac is currently under construction. It will be connected via the old UNILAC transfer beamline to SIS18 and has a length of ~30 m. The Linac will accelerate protons up to a final energy of 68 MeV at a pulse length of 35 μs and a maximum repetition rate of 4 Hz. It will operate at 325 MHz and consists of a new so called "Ladder" RFQ type, followed by a chain of CH-cavities, partially coupled by rf-coupling cells. We have worked out a diagnostics system, which allows detailed measurement and study of all beam parameters during commissioning and later during regular operation. The diagnostics devices will - in a first step - be installed on a diagnostics testbench for stepwise commissioning. We present the concepts for Linac and testbench with some special emphasis on energy measurements with spectrometer and Secondary Electron eMission (SEM-) grid profile measurements.

INTRODUCTION

The FAIR [1] facility at GSI is designed to provide antiproton and ion beams of worldwide unique intensity and quality for fundamental physics research.
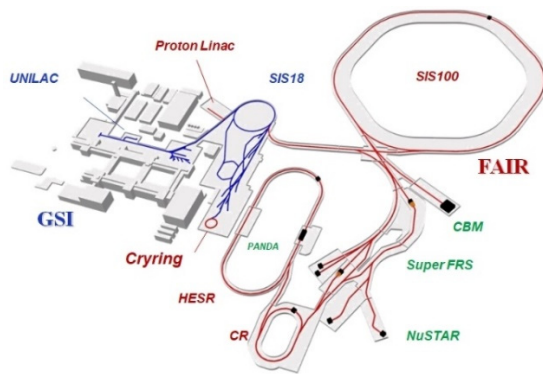

Figure 1: Layout of the FAIR facility.

The FAIR accelerator complex, shown in Fig. 1, will comprise three Linacs: the existing UNILAC (including a separate high charge state injector) a superconducting cw-Linac, designed mainly for intermediate energy experiments [2], and the new proton Linac [3] (pLinac). UNILAC and pLinac are the main injectors of SIS18, which is again an injector of the SIS100, the central accelerator component of FAIR.

---

†T.Sieber@gsi.de

The pLinac will deliver the beam for the antiproton chain. It will consist of an RFQ [4] followed by two 10 m sections of Cross Bar H-drifttube accelerator (CH) structures [5]. The first section includes six CH modules, which are pairwise rf-coupled (CCH). The second section consists of three separate modules, each one having its own klystron. The pLinac will deliver a beam current up to 70 mA at a macropulse length of 35 μs (max. 4 Hz) and a typical bunch length of 100 ps. The design energy is 68 MeV. Figure 2 shows a schematic of the proton Linac and associated beam instrumentation.
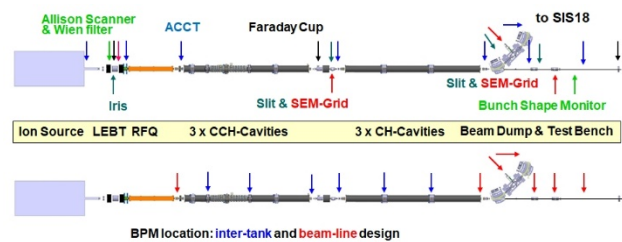

Figure 2: The FAIR proton Linac, showing the positions of the diagnostics elements (upper) and the BPMs (lower).

The overall diagnostics layout has been described elsewhere [6]. Due to the compact structure of the two CH sections, it will be concentrated in the LEBT, behind the RFQ (MEBT/rebuncher section) and in a diagnostics/rebuncher section between the CCH and CH accelerating sections. Beam diagnostics elements are placed also in the transfer line to SIS18 as well as in a straight line to the beam dump.

Special care had to be taken for the design of the SEM Grids. We expect a 1σ beam radius of 1.5 mm in the "worst case", therefore the wire pitch cannot be larger than 0.5 mm to obtain realistic profiles. Moreover, a stretching mechanism is required to compensate for thermal expansion, even if the grids are operated in a "grid protection mode" at reduced duty cycle. Any kind of plating on the tungsten wires must be considered carefully because of possible melting and agglutination during irradiation.

Concerning the testbench for stepwise Linac commissioning we want to measure longitudinal emittance at least for the first part, up to 35 MeV. The pLinac consists entirely of novel and innovative cavities, starting from a so-called ladder RFQ over the rf-coupled CCH cavities, to the CH tanks, both with KONUS particle dynamics. For that reason, a detailed step-by-step characterisation of each cavity is required and the testbench must be designed accordingly.

SEM GRID DESIGN

The working principle of SEM grids is based on secondary electrons, which are released from the grid wires upon ion beam impact. The resulting current distribution on an array of wires represents the beam profile in a given direction [7]. While grids cover both directions, harps cover only one coordinate axis. Due to the smaller size of the pLinac beam as compared to the UNILAC heavy ion beam, the traditional grid design of GSI only can only be used for the LEBT section. The LEBT SEM grid is made of 64 wires with 2.0 mm spacing for each plane. It is designed in a classical way, consisting of a frame with spring holders for each wire.

The grids for the Linac section (SD-section, inflection and dump), designed by PROACTIVE company in collaboration with GSI, will have a smaller wire spacing of 0.5 mm. The active area is 32 x 32 mm^2 corresponding to 64 wires for each plane. At the inflection and in the rebuncher (SD) section a grid for both transverse directions mounted on a pneumatic drive. However, at the dump and additionally in the SD section separate harps for the horizontal and vertical profiles are mounted on two stepping motor drives to allow for transverse emittance measurements in connection with two upstream slits. Table 1 shows the relevant parameters.

Table 1: Parameters of pLinac and SEM Grids

No. of Grids / Harps	2 / 4
No. of wires Grid / Harp	2 x 64 / 1 x 64
Wire pitch / diameter	0.5 mm / 100 μm
Wire material	Tungsten (gold plated)
Detection area	32 x 32 mm^2
Vacuum requirement	5*10^{-9} mbar (no bakeout)
Max. beam current	70mA
Pulse duration	10 – 100 μs
Repetition rate	1 – 4 Hz
Max. beam energy	68 MeV
Normal / max. grid temp.	2000 K / 3000 K

The mechanical design of the grid can be seen in Fig. 3. The structure is based on a PCB to which the wires are soldered on one side. On the other side, a specially designed stretching system is used to keep wires under tension during irradiation.

Besides high resolution and a compact design, special care has been taken for the field distribution due to the cleaning electrodes. These electrodes are kept at a positive potential to extract the secondary electrons and thus prevent them from being captured by neighbouring wires, which would deteriorate the measurement. The electric field distribution obtained with a parallel oriented diamond shaped electrode configuration is shown in Fig. 4. The potential required for the cleaning electrodes has been esti-

mated to be ~ 200 V. As can be seen, the electric field vanishes in the plane where the four (representative) wires are located. Consequently, a secondary electron generated at one of the wires and directed towards another one cannot be properly deterred from reaching it. This issue could generate unwanted crosstalk between the wires.
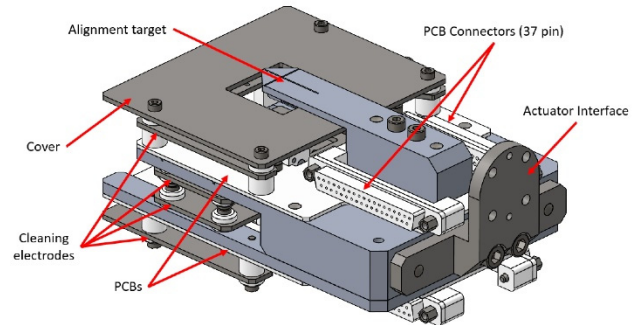

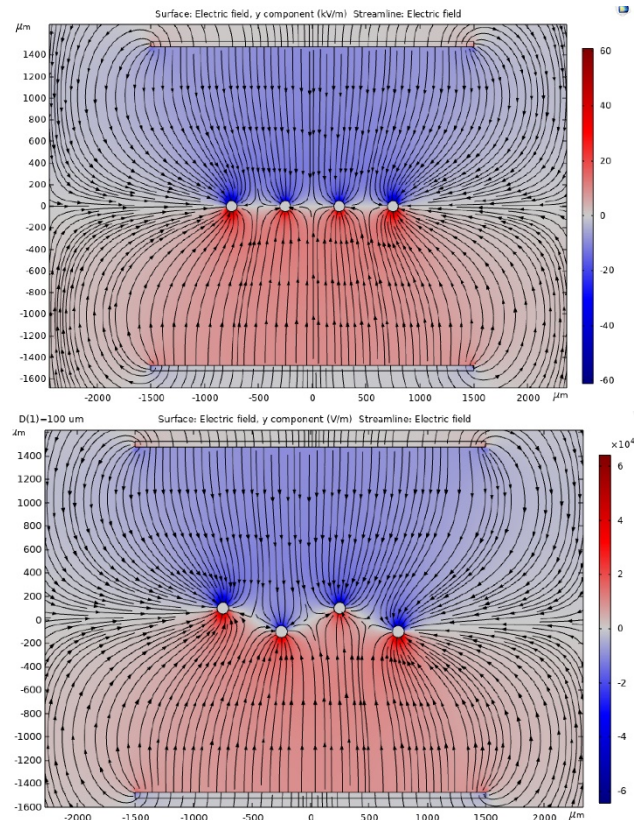Figure 3: SEM grid design by PROACTIVE.

Figure 4: Field distribution calculated for co-planar wires (upper). Field distribution with alternating wire positions (lower). The diamond shaped cleaning electrodes are located at top and bottom respectively.

In order to solve this issue, a new, non-planar disposition of the wires has been studied. The electric field distribution of this new design is also shown in Fig. 4. As can be seen,

with this new wire distribution the vanishing electric field plane is avoided, instead a rather sinusoidal shaped surface is observed on which the electric field vanishes. The electric field along a line joining two consecutive wires proves to be strongly repelling for electrons towards the ends of this line. A wire displacement of only 2/10 mm should provide a significant background reduction.

DIAGNOSTICS TESTBENCH

The testbench for stepwise commissioning will consist of all relevant types of diagnostic devices that have been developed for the pLinac and additionally a magnetic spectrometer for measurements of the proton beam's energy spread. A schematic overview of the planned bench is shown in Fig. 5.
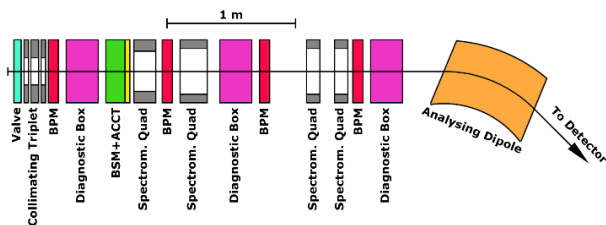

Figure 5: Schematic layout of the diagnostics testbench. The diagnostic boxes contain slits and/or grids. The sketch is longitudinally at scale.

A discussion of possible spectrometer designs is given in [8]. The main design goals are: the capability to work for proton energies from ≈ 3 up to ≈ 70 MeV, compatibility with the further testbench installation, low space demands especially to the side, since the distance from beam line to the tunnel's wall is only 2.5 m, good resolving power, cost effective realization with already available components. One of the proposed designs consists of magnetic quadrupole lenses and an analyzing dipole. These ion-optical elements fulfill two functions: to create a point-to-point image of the spectrometers input plane, at which a slit is placed, onto the spectrometer's output plane, at which a detector is placed, and to generate the dispersive effect needed for assessing the energy spectrum. The preliminary design presented in [8] uses four already available quadrupoles and one of the two 45° dipoles to eventually be placed at the end of the pLinac. It has a total length of approximately 6 m and extends roughly 1.7 m to the side. A first order estimate with 250 μm slit resulted in a resolution of 4000. However, as it turned out, its design had compatibility issues with the rest of the testbench.

Consequently, the design had to be modified. A schematic overview including the placement of all beam instrumentation devices to be part of the testbench is shown in Fig. 5. Since the input slit is positioned far from the RFQ's exit, a collimating quadrupole triplet has been added to the set-up. The triplet has the same design as those to be used between the RFQ and the CCH1 cavity. Besides, drift lengths and the field gradients had to be modified as compared to the preliminary design. Table 2 shows a comparison between the two sets of values. The present testbench

design has a length of about 5 m and extends approximately 1.8 m to the side. The spectrometer's resolving power remained practically unchanged.

Table 2: Spectrometer Design Comparison. Distances/Drifts are in mm, Quadrupole Gradients are in T/m and given for a Proton Energy of 3 MeV

Parameter	Old design	New design
RFQ to slit distance	125	704.8
slit to 1st quad drift	317	405
1st quad gradient	5.2	4.5
1st to 2nd quad drift	250	190
2nd quad gradient	2.12	2.4
2nd to 3rd quad drift	2000	777
3rd quad gradient	2.1	3.2
3rd to 4th quad drift	114	114
4th quad gradient	2.54	3.07
4th quad to dipole drift	500	750
dipole to detector drift	2040	2100

First order simulations performed with the GICOSY code [9] show that the proton beam can be properly guided over the whole length of the testbench while point-to-point imaging is ensured between the spectrometers input and output planes, see Fig. 6. Presently work is in progress to assess the influence of space charge and higher order effects.
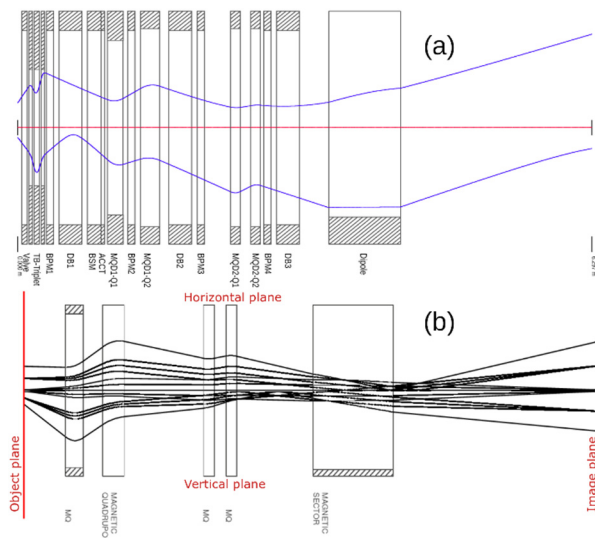

Figure 6: a) Beam envelopes in the horizontal and vertical planes, upper and lower half respectively. b) The point-to-point imaging feature of the spectrometer.

An alternative spectrometer design also discussed in [8] employs just two slits placed before the analyzing dipole and separated by an appropriate distance. This design is also under investigation and the testbench provides means for implementing it. Thus, an experimental comparison between the two designs is envisaged.

REFERENCES

[1] O. K. Kester, "Status of the FAIR Facility", in *Proc. 4th Int. Particle Accelerator Conf. (IPAC'13)*, Shanghai, China, May 2013, paper TUXB101, pp. 1085-1089.

[2] M. Miski-Oglu *et al.*, "Beam Commissioning of the Demonstrator Setup for the Superconducting Continuous Wave HIM/GSI-Linac", in *Proc. 10th Int. Particle Accelerator Conf. (IPAC'19)*, Melbourne, Australia, May 2019, pp. 33-36. doi:10.18429/JACoW-IPAC2019-MOZZPLM1

[3] L. Groening *et al.*, "Status of the FAIR 70 MeV Proton Linac", in *Proc. 26th Int. Linear Accelerator Conf. (LINAC'12)*, Tel-Aviv, Israel, Sep. 2012, paper THPB034, pp. 927-928.

[4] M. Schütt, U. Ratzinger, and R. Brodhage, "Proposal of a 325 MHz Ladder-RFQ for the FAIR Proton-Linac", in *Proc. 27th Int. Linear Accelerator Conf. (LINAC'14),* Geneva, Switzerland, Aug.-Sep. 2014, paper THPP071, pp. 1016-1018.

[5] G. Clemente *et al.*, "Development of room temperature cross-bar-H-mode cavities for proton and ion acceleration in the low to medium beta range", *Phys. Rev. ST Accel. Beams*, vol. 14, p. 110101, Nov. 2011.

doi:10.1103/physrevstab.14.110101

[6] T. Sieber *et al.*, "Beam Diagnostics Layout for the FAIR Proton Linac", in *Proc. 27th Int. Linear Accelerator Conf. (LINAC'14)*, Geneva, Switzerland, Aug.-Sep. 2014, paper THPP063, pp. 998-1000.

[7] P. Forck, "Lecture Notes on Beam Instrumentation and Diagnostics", Joint University Accelerator School (JUAS), Darmstadt, Germany, Jan.-Mar. 2011.

[8] S. Udrea *et al.*, The Beam Diagnostics Test Bench for the Commissioning of the Proton Linac at FAIR", In *Proc. 8th Int. Beam Instrumentation Conf. (IBIC'19)*, Sep. 2019, p. 196. doi:10.18429/JACoW-IBIC2019-MOPP038

[9] GICOSY, https://webdocs.gsi.de/~weick/gicosy/.